

Journal of Mechanics of Materials and Structures

CONTOURS FOR PLANAR CRACKS GROWING IN THREE DIMENSIONS

Louis Milton Brock

Volume 10, No. 1

January 2015



CONTOURS FOR PLANAR CRACKS GROWING IN THREE DIMENSIONS

LOUIS MILTON BROCK

A three-dimensional dynamic steady state analysis for extension of a semi-infinite plane crack is considered. Fracture is brittle and driven by loads applied to the crack surfaces. An analytical solution is obtained, and examined in light of two criteria: energy release (rate) and strain energy density. Introduction of a quasipolar coordinate system allows, for each criterion, generation of a nonlinear first-order differential equation for the distance from the origin to any point on the crack edge. These in turn give insight into the crack contour generated by the crack edge. In particular, for loading by compressive point forces, the equation generated by the energy release (rate) criterion is solved exactly. Calculations depict a crack edge contour that tends to the rectilinear, but deviates markedly from that near the point forces.

Introduction

The author considers sliding contact in the 3D dynamic steady state by rigid dies in [Brock 2012; 2014a; 2014b; 2015]. Basic die shapes — sphere, ellipsoid, cone — are treated [Brock 2012; 2014a], but also more complicated shapes [Brock 2014a; 2014b; 2015] that preclude simple connectivity of the contact zone [Brock 2014b] or a single contact zone [Brock 2015]. These 3D studies demonstrate the sensitivity of contact zone contour to sliding speed, and show that contact zone shape does not necessarily replicate the projection of the die profile onto the half-space.

An analogous goal in fracture mechanics is to determine crack edge location. In 2D dynamic fracture, this requires an equation of motion for the crack tip [Freund 1990]. In a 3D study, such an equation must describe the crack contour defined by crack edge location. The paper, therefore, considers semi-infinite crack growth in an unbounded solid. For simplicity, the crack is assumed to (a) remain in its original plane, (b) be driven by crack surface loads that translate at constant subcritical speed in a fixed direction and (c) achieve a dynamic steady state.

While analogous, the study does not enjoy some features of [Brock 2012; 2014a; 2014b; 2015]: (a) die/half-space conformation is paramount in defining the solution, (b) the (valid) assumption of a “small” contact zone often allows conformation to be expressed in terms of polynomials and (c) solution of the conformation equation itself can be simplified under the same assumption, e.g. [Brock 2014a]. Prescribed geometrical properties do not in general define fracture criteria. Indeed, geometrical features (crack edge location, crack contour) are outputs. Therefore, approximations for the equation of crack edge location may be unrealistic.

The 3D analysis begins by considering the unmixed boundary value problem for a displacement discontinuity imposed over a semi-infinite plane area A_C contained in an unbounded solid. The discontinuity vanishes along area boundary C , vanishes at infinite distances from it, and translates with A_C at constant subcritical speed V in a fixed direction. A dynamic steady state ensues and allows use of a translating

Keywords: 3D, dynamic, criteria, analytic solution, crack edge contour, crack edge location.

Cartesian basis. The transform solution is generated, but a quasipolar coordinate system is introduced in the inversion process. Expressions for traction on the plane of A_C lead to classical singular integral equations for the displacement discontinuity produced were A_C a crack subject to prescribed surface loads. Two fracture criteria are considered, and each leads to a nonlinear first-order differential equation for the distance from a fixed point in A_C to any point on (now) crack edge C .

Displacement discontinuity growth — governing equations

Consider an unbounded, isotropic and linearly elastic solid. In terms of Cartesian basis $\mathbf{x} = \mathbf{x}(x_k)$, semi-infinite planar region ($x_3 = 0, x_1 < 0$) A_C is subject to discontinuity

$$[\mathbf{u}(u_k)] = \mathbf{U}(U_k). \quad (1)$$

Here $k = (1, 2, 3)$, $[\]$ signifies a jump as travel from $x_3 = 0^-$ to $x_3 = 0^+$ occurs, \mathbf{u} is the displacement field and $U_k = U_k(x_1, x_2)$ discontinuity components. Region extension then occurs in the positive x_1 -direction with constant subcritical speed V . A dynamic steady state is achieved such that \mathbf{U} does not change, and region boundary C assumes a fixed, albeit no longer rectilinear, profile. Displacement $\mathbf{u}(u_k)$ and traction $\mathbf{T}(\sigma_{ik})$ are invariant in the moving frame of A_C . Basis \mathbf{x} is therefore translated with A_C so that $u_k = u_k(\mathbf{x})$, $U_k = U_k(x_1, x_2)$, $\sigma_{ik} = \sigma_{ik}(\mathbf{x})$ and the time derivative can be written as $-V\partial_1$. Here ∂_k signifies x_k -differentiation. For convenience $\mathbf{x} = 0$ is located in the dislocation region, so that function $\mathfrak{S}(x_1, x_2) = 0$, $\sqrt{x_1^2 + x_2^2} \neq 0$ defines contour C and the region can be defined as $(x_1, x_2) \in A_C$. Both \mathfrak{S} and its gradient $\nabla\mathfrak{S}$ are continuous, and any line passing through $\mathbf{x} = 0$ in the x_1x_2 -plane can cross C only once. For $x_3 \neq 0$, governing equations for $\mathbf{u}(x_k)$ can be written as [Brock 2012]

$$\mathbf{u} = \mathbf{u}_D + \mathbf{u}_S, \quad (2a)$$

$$(\nabla^2 - c^2\partial_1^2)\mathbf{u}_S = 0, \quad \nabla \cdot \mathbf{u}_S = 0, \quad (2b)$$

$$(c_D^2\nabla^2 - c^2\partial_1^2)\mathbf{u}_D = 0, \quad \nabla \times \mathbf{u}_D = 0. \quad (2c)$$

In (2) ∇^2 is the Laplacian, and traction \mathbf{T} is defined by

$$\frac{1}{\mu}\mathbf{T} = [(c_D^2 - 2)\nabla \cdot \mathbf{u}_D]\mathbf{1} + 2(\nabla\mathbf{u} + \mathbf{u}\nabla). \quad (3)$$

Term $\mathbf{1}$ is the identity tensor, and (c, c_D) are dimensionless ratios

$$c = \frac{V}{V_S}, \quad c_D = \frac{V_D}{V_S}. \quad (4)$$

Here (V, V_S, V_D) are, respectively, translation speed, shear wave speed, and dilatational wave speed, where

$$c_D = \sqrt{2\frac{1-\nu}{1-2\nu}}, \quad V_S = \sqrt{\frac{\mu}{\rho}}. \quad (5)$$

In (2)–(5), (ν, μ, ρ) are Poisson's ratio, shear modulus and mass density, and $1 < c_D$. In light of (1),

conditions for $x_3 = 0$ are

$$[u_k] = U_k(x_1, x_2) \in A_C, \quad [u_k] = 0(x_1, x_2) \notin A_C, \quad (6a)$$

$$[\sigma_{3k}] = 0. \quad (6b)$$

Components U_k are not specified, but must be finite and continuous for $(x_1, x_2) \in A_C$. Therefore $U_k = 0$ for $\mathfrak{S}(x_1, x_2) = 0$, and (\mathbf{u}, \mathbf{T}) should remain finite for $|\mathbf{x}| \rightarrow \infty, x_3 \neq 0$.

General transform solution

A double bilateral transform [Sneddon 1972] can be defined as

$$\hat{F} = \iint F(x_1, x_2) \exp(-p_1 x_1 - p_2 x_2) dx_1 dx_2. \quad (7)$$

Integration is along the entire $\text{Re}(x_1)$ and $\text{Re}(x_2)$ -axes. Application of (7) to (2) gives

$$\hat{\mathbf{u}}_S = \mathbf{V} \exp(-B|x_3|), \quad \hat{\mathbf{u}}_D = \mathbf{U} \exp(-A|x_3|), \quad (8a)$$

$$p_1 V_1 + p_2 V_2 - B V_3 = 0, \quad \mathbf{U} = (p_1, p_2, -A)\mathbf{U}. \quad (8b)$$

Terms (B, A) are roots of the transforms of, respectively, (2b) and (2c), given by

$$B = \sqrt{-D + c^2 p_1^2}, \quad A = \sqrt{-D + (c^2/c_D^2) p_1^2}, \quad D = p_1^2 + p_2^2. \quad (9)$$

Equation (8) is bounded for $x_3 \neq 0$ if branch cuts are introduced so that $\text{Re}(B, A) \geq 0$ in the cut complex (p_1, p_2) -planes. Application of (7) to (6) and substitution of (8) and (9) gives equations for (U, V_1, V_2) in terms of transforms \hat{U}_k . The solutions for $x_3 \geq 0(+)$ and $x_3 \leq 0(-)$ are given by (A.1). Expressions for traction $(\sigma_{33}, \sigma_{31}, \sigma_{32})$ in plane $x_3 = 0$ are also required and, in light of (3), (7) and (A.1), their transforms are given by (A.3).

Transform inversion — general formulas

In (6), inhomogeneous terms (U_1, U_2, U_3) arise only for $(x_1, x_2) \in A_C$. In light of (A.3), therefore, the inversion operation corresponding to (7) gives $(\sigma_{33}, \sigma_{31}, \sigma_{32})$ for $x_3 = 0$ as linear combinations of expressions

$$\iint U_k d\xi_1 d\xi_2 \frac{1}{2\pi i} \int dp_1 \frac{1}{2\pi i} \int P_k dp_2 \exp[p_1(x_1 - \xi_1) + p_2(x_2 - \xi_2)]. \quad (10)$$

Here $U_k = U_k(\xi_1, \xi_2)$ and $P_k = P_k(p_1, p_2)$ is the corresponding coefficient. Double integration is over region A_C , and single integration is over the entire $\text{Im}(p_1)$ and $\text{Im}(p_2)$ -axes. The form of (10) suggests definitions and transformations [Brock 2012]:

$$p_1 = p \cos \psi, \quad p_2 = p \sin \psi, \quad (11a)$$

$$\begin{bmatrix} x \\ y \end{bmatrix} = \begin{bmatrix} \cos \psi & \sin \psi \\ -\sin \psi & \cos \psi \end{bmatrix} \begin{bmatrix} x_1 \\ x_2 \end{bmatrix}, \quad \begin{bmatrix} \xi \\ \eta \end{bmatrix} = \begin{bmatrix} \cos \psi & \sin \psi \\ -\sin \psi & \cos \psi \end{bmatrix} \begin{bmatrix} \xi_1 \\ \xi_2 \end{bmatrix}. \quad (11b)$$

In (11), $\text{Re}(p) = 0+$, $|\text{Im}(p), x, y, \xi, \eta| < \infty$ and $|\psi| < \pi/2$. Parameters (p, ψ) , $(x, \psi; y = 0)$ and $(\xi, \psi; \eta = 0)$ resemble quasipolar coordinate systems, i.e.,

$$d\xi_1 d\xi_2 = |\xi| d\xi d\psi, \quad dp_1 dp_2 = |p| dp d\psi. \quad (12)$$

Use of (11) and (12) in (9) and (A.3) give

$$D = p^2, \quad B = B\sqrt{-p^2}, \quad A = A\sqrt{-p^2}, \quad K = Kp^2, \quad (13a)$$

$$B = \sqrt{1 - c^2 \cos^2 \psi}, \quad A = \sqrt{1 - (c^2/c_D^2) \cos^2 \psi}, \quad K = c^2 \cos^2 \psi - 2. \quad (13b)$$

In light of (7) and conditions for contour function \mathfrak{S} , (10) assumes the form

$$\frac{1}{i\pi} \int_{\Psi} P_k d\psi \int_N d\eta \frac{\partial}{\partial x} \int_X d\xi \frac{\partial U_k}{\partial \xi}(\xi, \eta) \frac{1}{2\pi i} \int \frac{|p| \sqrt{-p}}{p \sqrt{p}} dp \exp(p(x - \xi)). \quad (14)$$

Symbols (N, X, Ψ) signify integration over ranges $|\psi| < \pi/2$, $N^- < \eta < N^+$ and $X_- < \psi < X_+$, respectively. Here $P_k = P_k(\psi)$, and p -integration is along the positive side of the entire imaginary axis. Terms in (8) are bounded for positive and real (B, A) if branches $\text{Im}(p) = 0$, $\text{Re}(p) < 0$ and $\text{Im}(p) = 0$, $\text{Re}(p) > 0$ are introduced for $\sqrt{\pm p}$, respectively, such that $\text{Re}(\sqrt{\pm p}) > 0$ in the cut p -plane. The p -integration is given in Appendix B so that, in view of the condition that U_k vanish continuously on C [Brock 2012],

$$\frac{1}{\pi} \int_{\Psi} P_k d\psi \frac{\partial}{\partial x} \int_N d\eta \frac{1}{\pi} \int_X \frac{\partial U_k}{\partial \xi}(\xi, \eta) \frac{d\xi}{\xi - x}. \quad (15)$$

Limits $N^{\pm}(\psi)$ in (15) are defined by

$$\mathfrak{S}(\xi_1(\xi, N^{\pm}), \xi_2(\xi, N^{\pm})) = 0, \quad \frac{dN^{\pm}}{d\xi} = 0. \quad (16)$$

That is, for given ψ , limits N^{\pm} are the maximum and minimum values of η on C , and for given η , limits $X_{\pm}(\psi, \eta)$ locate the ends of lines that run parallel to the ξ -axis and that span C . Conditions on C imply that these limits exist, are single-valued, and vary continuously in ψ . In particular, the semi-infinite nature of A_C guarantees that $X_- \rightarrow -\infty$ for portions of Ψ . Figure 1 gives a generic sketch of A_C for the case that $N^+(\psi) \rightarrow \infty$ and $|X_-(\psi, \eta)|$ is finite but too large to appear.

In light of (7)–(13), traction in A_C itself, i.e., $x_3 = 0$, $(x_1, x_2) \in A_C$, can be written as

$$\sigma_{3k} = -\frac{1}{\pi} \int_{\Psi} d\psi \int_N d\eta \frac{\partial}{\partial x} \int_X d\xi \delta(\xi, \eta) \sigma_{3k}(x_1(\xi, \eta), x_2(\xi, \eta)). \quad (17)$$

In (17), δ is the Dirac function. Therefore, expressions for traction in A_C can be obtained by matching the integrands of (ψ, η) -integration in (17) with combinations of those in (15). Moreover, ξ in (15) and (17) is an integration variable representing parameter x that itself depends on (x_1, x_2) and ψ . As noted in connection with (11), coordinates (x_1, x_2) can be replaced by (x, ψ) for $y = 0$. Thus every point $(x_1, x_2) \in A_C$ lies on an integration path $\eta = 0$ that passes through both limit points of the ξ -integral. The resulting expressions for traction in A_C are given in Appendix C. Equation (13b) shows that (B, A) are positive and real so long as $c < 1$. Term R in (C.3) is the Rayleigh function [Achenbach 1975] of argument $c \cos \psi$ and vanishes at value $c \cos \psi = c_R$ ($0 < c_R < 1$) where $V_R = c_R V_S$ is the Rayleigh wave

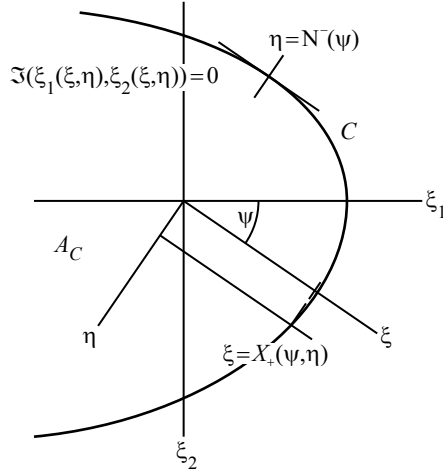


Figure 1. Schematic of semi-infinite area A_C and contour C .

speed. To avoid critical behavior, therefore, the translation speed of C is subject to restriction $0 < c < c_R$. Crack extension in the dynamic steady state can now be treated. The treatment begins with some basic results for extension caused by crack surface traction.

Related crack extension problem: basic results

Region A_C in the dynamic steady state is now a crack whose two surfaces are subjected to traction $(-\sigma_{33}^C, -\sigma_{31}^C, -\sigma_{32}^C)$, with $\sigma_{3k}^C > 0$. Crack geometry, i.e., C , $\mathfrak{S}(x_1, x_2) = 0$ and V , is the same as before. The conditions placed on U_k above are relevant for fracture. In light of 2D dynamic steady state analyses of semi-infinite cracks [Brock 1999] therefore, $(\sigma_{33}^C, \sigma_{31}^C, \sigma_{32}^C)$ must be finite and piecewise continuous. Behavior should also be such that, for $(x_1, x_2) \in A_C$,

$$\sigma_{3k}^C \approx O((x_1^2 + x_2^2)^{-\chi}), \quad \sqrt{x_1^2 + x_2^2} \rightarrow \infty \quad (\chi > 1). \quad (18)$$

Coupled singular integral equations for x -derivatives of (now-unknown) components (U_1, U_2, U_3) are provided by (C.3), with σ_{3k} replaced by $-\sigma_{3k}^C$. Solution gives the derivatives and the functions themselves. To emphasize aspects of 3D behavior, σ_{3k}^C -values are maximum near $(x_1, x_2) = 0$. It is then reasonable to assume that any curvature of crack edge C will produce an essentially concave profile with respect to $(x_1, x_2) = 0$. In view of the original restrictions on C , then, two cases arise. For $X_+ = x_+(\psi) > 0$, $X_- = -x_-(\psi)$,

$$\frac{\partial U_k}{\partial x} = \frac{1}{\sqrt{x_+ - x} \sqrt{x + x_-}} \frac{(\text{vp})}{\pi} \int_X \frac{g_k(\xi, \psi)}{\xi - x} \sqrt{x_+ - \xi} \sqrt{\xi + x_-} d\xi, \quad (19a)$$

$$U_k = \frac{1}{\pi} \int_X g_k(\xi, \psi) \ln \left| \frac{\sqrt{x_+ - x} \sqrt{\xi + x_-} - \sqrt{x + x_-} \sqrt{x_+ - \xi}}{\sqrt{x_+ - x} \sqrt{\xi + x_-} + \sqrt{x + x_-} \sqrt{x_+ - \xi}} \right| d\xi. \quad (19b)$$

Continuity of C requires that $x_{\pm}(\pi/2) = x_{\mp}(-\pi/2)$. For $X_+ = x_+(\psi)$, $X_- \rightarrow -\infty$,

$$\frac{\partial U_k}{\partial x} = \frac{1}{\sqrt{x_+ - x}} \frac{(\text{vp})}{\pi} \int_X \frac{g_k(\xi, \psi)}{\xi - x} \sqrt{x_+ - \xi} d\xi, \quad (20a)$$

$$U_k = \frac{1}{\pi} \int_X g_k(\xi, \psi) \ln \left| \frac{\sqrt{x_+ - \xi} - \sqrt{x_+ - x}}{\sqrt{x_+ - \xi} + \sqrt{x_+ - x}} \right| d\xi. \quad (20b)$$

Continuity of C now requires that $x_+(\pm\pi/2) \rightarrow \infty$. Equations (19b) and (20b) vanish continuously on C , as required. In (19) and (20),

$$g_1 = \frac{1}{N} \left[\frac{M}{B} \left(\frac{\sigma_{32}^C}{\mu} \cos \psi - \frac{\sigma_{31}^C}{\mu} \sin \psi \right) \sin \psi - \frac{\sigma_{31}^C}{\mu} B c^2 \cos^2 \psi \right], \quad (21a)$$

$$g_2 = \frac{1}{N} \left[\frac{M}{B} \left(\frac{\sigma_{32}^C}{\mu} \sin \psi - \frac{\sigma_{12}^C}{\mu} \cos \psi \right) \cos \psi - \frac{\sigma_{32}^C}{\mu} B c^2 \cos^2 \psi \right], \quad (21b)$$

$$g_3 = -\frac{2A}{R} \frac{\sigma_{33}^C}{\mu} c^2 \cos^2 \psi. \quad (21c)$$

Substitution of (19a) and (20a) into (15), but then performing the ξ -integration for $x \notin X$ leads to, respectively, expressions for traction on plane $x_3 = 0$, $(x, \psi) \notin A_C$,

$$\sigma_{3k} = \frac{1}{\pi \sqrt{x_+ - x} \sqrt{x_- + x}} \int_X \frac{\sigma_{3k}^C(\xi, \psi)}{\xi - x} \sqrt{x_+ - \xi} \sqrt{\xi + x_-} d\xi, \quad (22a)$$

$$\sigma_{3k} = \frac{1}{\pi \sqrt{x_+ - x}} \int_X \frac{\sigma_{3k}^C(\xi, \psi)}{\xi - x} \sqrt{x_+ - \xi} d\xi. \quad (22b)$$

Brittle fracture parameter: energy release (rate)

After [Griffith 1921], crack growth occurs when the rate of surface energy release balances that of potential energy decrease. For the 2D brittle crack, this criterion equates the rate per unit length (of crack edge) of energy release and negative of power per unit length generated in the crack plane [Achenbach 1975; Freund 1990]. Here, total release rate \mathfrak{R} and total power are considered. Use of (8) for the dynamic steady state gives

$$\mathfrak{R} = -V \int_{\Psi} d\psi \left[\int_{-\infty}^{\infty} |x| dx \sigma_{3k} \partial_1 U_k + \int_X |x| dx \sigma_{3k}^C \partial_1 U_k \right], \quad (23a)$$

$$\partial_1 = \cos \psi \frac{\partial}{\partial x} - \frac{\sin \psi}{|x|} \frac{\partial}{\partial \psi}, \quad \partial_2 = \sin \psi \frac{\partial}{\partial x} + \frac{\cos \psi}{|x|} \frac{\partial}{\partial \psi}. \quad (23b)$$

The summation convention is understood in (23a). To illustrate the form of \mathfrak{R} , the ∂_1 -operator is applied to case (20b) as

$$\begin{aligned} \partial_1 U_k = & -\frac{(\text{vp})}{\pi \sqrt{x_+ - x}} \int_X g_k d\xi \left[\frac{\sqrt{x_+ - \xi}}{\xi - x} \cos \psi - \frac{\sin \psi}{|x| \sqrt{x_+ - \psi}} \frac{dx_+}{d\psi} \right] \\ & + \frac{\sin \psi}{\pi |x|} \int_X d\xi \ln \left| \frac{\sqrt{x_+ - \xi} + \sqrt{x_+ - x}}{\sqrt{x_+ - \xi} - \sqrt{x_+ - x}} \right| \frac{\partial g_k}{\partial \psi}. \end{aligned} \quad (24)$$

The x -integration sum, (17), (19b), (22b) and (24) imply that $\mathfrak{R} = 0$ in (23a). But in the sense of a distribution each term in the sum gives [Achenbach and Brock 1973]

$$\frac{H(x_+ - x)}{\sqrt{x_+ - x}} \frac{H(x - x_+)}{\sqrt{x - x_+}} = \frac{\pi}{2} \delta(x - x_+). \quad (25)$$

Here H is the step function. Also, \mathfrak{R} is assumed invariant with respect to its integrand in (23a). Singular behavior guarantees invariance in terms of x , so that the integrand need only be constant in terms of ψ . Therefore, for $|\psi| < \pi/2$,

$$\frac{\mathfrak{R}}{\sqrt{\mu\rho}} = \frac{-c}{\pi} \frac{d}{x_+ d\psi} (x_+ \sin \psi) \int_X \frac{\sigma_{3k}^C d\xi}{\mu\sqrt{x_+ - \xi}} \int_X \frac{g_k d\xi}{\sqrt{x_+ - \xi}}. \quad (26)$$

Equation (26) is, in effect, a nonlinear differential equation for $x_+(\psi)$. Equation (26) is based on (20). Thus for $|\psi| = \pi/2$, $x_+ \rightarrow \infty$ yet \mathfrak{R} is invariant and finite. For $|\psi| \approx \pi/2$, Equations (13b), (18), (21), (C.3) and (26) lead to asymptotic forms

$$\int_X \frac{\sigma_{3k}^C(t, \psi)}{\sqrt{x_+ - t}} dt \approx -\frac{\Sigma_{3k}}{x_+^{\chi-1/2}} G_\chi, \quad G_\chi = \int_{-1}^{\infty} \frac{du}{u^\chi \sqrt{1+u}}, \quad (27a)$$

$$\frac{\mathfrak{R}}{\sqrt{\mu\rho}} \approx \frac{c}{8\pi^2} \frac{G_\chi^2}{x_+^{2\chi}} \frac{dx_+}{d\psi} \left(\frac{c_D^2}{c_D^2 - 1} \Sigma_{33}^2 + \Sigma_{31}^2 - \Sigma_{32}^2 \right). \quad (27b)$$

It is noted that the right-hand side of (27b) is finite when $x_+ \approx O(1/\sqrt{\cos \psi})$ for $|\psi| \approx \pi/2$ and $\chi = \frac{3}{2}$. It is also to be noted that for $\psi = 0$, (26) in fact involves only $x_+(0)$ itself.

Brittle fracture parameter: strain energy density

Another brittle fracture model [Sih 1973] posits that an edge segment of a stationary crack will extend in a given direction if the strain energy density E achieves a maximum in that direction, where

$$\frac{E}{\mu} = \frac{c_D^2}{2} \varphi_1 - 2\varphi_2, \quad (28a)$$

$$\varphi_1 = e_{11} + e_{22} + e_{33}, \quad \varphi_2 = e_{11}e_{22} + e_{22}e_{33} + e_{33}e_{11} - e_{12}^2 - e_{23}^2 - e_{31}^2. \quad (28b)$$

Equation (28b) gives the first and second invariant of strain, where $2e_{ik} = \partial_i u_k + \partial_k u_i$. Behavior near the crack edge, i.e., distance $r \rightarrow 0$, for brittle fracture, is

$$E \approx \frac{S}{r}. \quad (29)$$

Therefore S is the key parameter. In keeping with the study of energy release rate, we examine the strain energy W itself in a thin “tube” that encases crack edge C . This value is infinite, but the result obtained below will correspond to (28). Results for $x_3 \neq 0$ are now required. In view of (7)–(14) and (A.1),

components of $\partial u_k/\partial x$ can be written as real or imaginary parts of a complex form as

$$\frac{1}{i\pi} \int_{\Psi} d\psi \int_N d\eta \frac{\partial}{\partial x} \int_X d\xi \frac{\partial U_k}{\partial \xi}(\xi, \eta) \frac{1}{2\pi i} \int \frac{|p|}{p} \left[P_k \frac{\sqrt{-p}}{\sqrt{p}} + i Q_k \right] dp \times \exp(p(x - \xi) - \sqrt{-p}\sqrt{p}\Omega|x_3|). \quad (30)$$

Symbol Ω represents (A, B) defined by (13b). The p -integration is obtained from Appendix B. Use of (20a) and a result corresponding to (17) gives generic form

$$\frac{1}{\pi^2} \int_X g_k dt \sqrt{x_+ - t} \frac{1}{\pi} \int_X \frac{d\xi}{(t - \xi)\sqrt{\xi - x_+}} \frac{P_k + i Q_k}{x - \xi - i\Omega|x_3|}. \quad (31)$$

The ξ -integration is performed by residue theory. Integration of (31) with respect to x , in view of the condition that u_k vanish on C , gives a generic form for u_k -components

$$-\frac{1}{\pi^2} (P_k + i Q_k) \int_X g_k \ln \frac{\sqrt{P} - \sqrt{x_+ - t}}{\sqrt{P} + \sqrt{x_+ - t}} dt, \quad P = x - x_+ - i\Omega|x_3|. \quad (32)$$

Equation (28b) requires ∇u_k , and (11) shows that x_k -dependence in (32) is bound up in P which, for case $\Omega = A$, is

$$P = r_A \exp(i\phi_A), \quad (33a)$$

$$r_A = \sqrt{(x - x_+)^2 + A^2 x_3^2}, \quad \phi_A = \tan^{-1} \frac{A x_3}{x - x_+} \quad (|\phi_A| < \pi). \quad (33b)$$

Knowledge of ∇u_k near C suffices for (29), so, for $\Omega = A$, (32) can be replaced with the asymptotic result

$$\frac{1}{\pi^2} (P_k + i Q_k) \int_X \frac{g_k dt}{\sqrt{x_+ - t}} \sqrt{r_A} \exp\left(i \frac{\phi_A}{2}\right) + O(r_A). \quad (34)$$

This form suggests that for given ψ a standard polar coordinate system (r, ϕ) , centered on C , be defined in the $x - x_3$ plane with

$$r = \sqrt{(x - x_+)^2 + x_3^2} \quad (r \approx 0), \quad \phi = \tan^{-1} \frac{x_3}{x - x_+} \quad (|\phi| < \pi). \quad (35)$$

Operations $(\partial_1, \partial_2, \partial_3)$ on (34) required for ∇u_k follow, respectively, in view of (11), (23b), (33) and (35), as

$$\frac{-1}{\pi^2 A_\Phi \sqrt{2r}} (P_k + i Q_k) \int_X \frac{g_k dt}{\sqrt{x_+ - t}} [A_+ + i A_- \operatorname{sgn}(\phi)] \frac{d}{x_+ d\psi} (x_+ \sin \psi), \quad (36a)$$

$$\frac{1}{\pi^2 A_\Phi \sqrt{2r}} (P_k + i Q_k) \int_X \frac{g_k dt}{\sqrt{x_+ - t}} [A_+ + i A_- \operatorname{sgn}(\phi)] \frac{d}{x_+ d\psi} (x_+ \cos \psi), \quad (36b)$$

$$\frac{i A}{\pi^2 A_\Phi \sqrt{2r}} (P_k + i Q_k) \int_X \frac{g_k dt}{\sqrt{x_+ - t}} [A_+ + i A_- \operatorname{sgn}(\phi)] \operatorname{sgn}(\phi). \quad (36c)$$

The result for $\Omega = B$ follows by replacing (A_{\pm}, A_{Φ}) with (B_{\pm}, B_{Φ}) , where

$$A_{\Phi} = \sqrt{1 - (c^2/c_D^2) \cos^2 \psi \sin^2 \phi}, \quad A_{\pm} = \sqrt{A_{\Phi} \pm \cos \phi}, \quad (37a)$$

$$B_{\Phi} = \sqrt{1 - c^2 \cos^2 \psi \sin^2 \phi}, \quad B_{\pm} = \sqrt{B_{\Phi} \pm \cos \phi}. \quad (37b)$$

Derivatives with respect to ψ , it is noted, for (P_k, Q_k, g_k) , (A_{\pm}, A_{Φ}, A) and (B_{\pm}, B_{Φ}, B) in (34) are associated with terms that vanish as $r \rightarrow 0$; see (24). To illustrate the results of (36), strain components for the case of pure crack surface compression ($\sigma_{31}^C = \sigma_{32}^C = 0$) are given in Appendix D. Equations (28), (29), (36) and (D.1) show that

$$E \approx \frac{1}{r} \Sigma(\psi, \phi). \quad (38)$$

In view of (21), therefore, $\Sigma(\psi, \phi)$ is quadratic in

$$\int_X \frac{\sigma_{3k}^C dt}{\sqrt{x_+ - t}}, \quad \frac{d}{x_+ d\psi}(x_+ \sin \psi), \quad \frac{d}{x_+ d\psi}(x_+ \cos \psi). \quad (39)$$

Strain energy W in a thin tube ($r \approx 0$) that encases crack edge C can be written as

$$W = r \int_{\Phi} d\phi \int_{\Psi} \Sigma(\psi, \phi) dC(\psi), \quad dC(\psi) = \sqrt{x_+^2 + (dx_+/d\psi)^2} d\psi. \quad (40)$$

Symbol Φ signifies integration over range $|\phi| < \pi$ and $dC(\psi)$ is the increment of length along the crack edge. If W is assumed to be invariant, a critical strain energy density parameter for $|\psi| < \pi/2$ is

$$\frac{\partial^2 W}{\partial r \partial \psi} = S_C = \int_{\Phi} \Sigma(\psi, \phi) d\phi \sqrt{x_+^2 + (dx_+/d\psi)^2}. \quad (41)$$

While more complicated than energy release rate \mathfrak{R} given by (26), (41) is in effect also a nonlinear differential equation for crack edge geometry parameter $x_+(\psi)$. Equation (40) is also based on (20), and for $|\psi| \approx \pi/2$, (37) gives

$$\left(\frac{A_+}{A_{\Phi}}, \frac{B_+}{B_{\Phi}} \right) = \sqrt{2} \cos \frac{\phi}{2}, \quad \left(\frac{A_-}{A_{\Phi}}, \frac{B_-}{B_{\Phi}} \right) = \sqrt{2} \left| \sin \frac{\phi}{2} \right|. \quad (42)$$

A standard table is used to carry out integration in (41). Use of (27a), (28), (D.1) and (D.2) lead to the asymptotic formula

$$S_C \approx \frac{1}{2\mu} \left[\frac{G_{\chi} \Sigma_{33}}{\pi^2 (c_D^2 - 1)} \right]^2 \frac{dx_+}{d\psi} \left[c_D^2 (2 - \pi c_D^2) + \frac{\pi}{2} \left(\frac{dx_+}{x_+ d\psi} \right)^2 \right]. \quad (43)$$

If asymptotic traction behavior ($\chi = \frac{3}{2}$) featured with (27b) is imposed, (43) gives finite S_C for $|\psi| = \pi/2$ when $x_+ \approx O(1/\cos^2 \psi)$ as $|\psi| \rightarrow \pi/2$. In addition, (D.1) shows that S_C does not give an algebraic equation for $x_+(0)$; see (26).

Illustration: application of energy release (rate) criterion

The strain energy density criterion is generally applied to static situations to ascertain the (possibly) out-of-plane direction that a crack edge segment may move [Sih 1973]. Therefore, planar crack edge behavior

ψ	0°	5°	15°	30°	45°	60°	75°	85°	90°
$c = 0.1$	1.0	0.989	0.95	0.912	0.932	1.051	1.406	2.187	∞
$c = 0.4$	1.0	0.987	0.936	0.881	0.887	0.987	1.319	2.238	∞

Table 1. Ratio $\frac{x_+(\psi)}{x_+(0)}$ for various (c, ψ) .

in the dynamic steady state is illustrated here in terms of the energy release (rate) criterion. For simplicity,

$$\sigma_{31}^C = \sigma_{32}^C = 0, \quad \sigma_{33}^C = \frac{P\delta(r_0)}{2\pi r_0}, \quad r_0 = \sqrt{x_1^2 + x_2^2}. \quad (44)$$

Here P is a force, so that traction σ_{33}^C is the axially symmetric Dirac function in standard polar coordinates. In view of (21) and (42), criterion (26) reduces to (see (D.2))

$$\frac{\mathfrak{R}}{\sqrt{\mu\rho}} = \frac{2A}{\pi R} \left(\frac{G}{u}\right)^2 c^3 \cos^2 \psi \frac{d}{x_+ d\psi} (x_+ \sin \psi), \quad G = \int_X \frac{\sigma_{33}^C dt}{\sqrt{x_+ - t}}. \quad (45)$$

The expression for G is found in Appendix E, and so (45) gives differential equation

$$\frac{\mathfrak{R}}{\sqrt{\mu\rho}} = \left(\frac{P}{2\pi\mu}\right)^2 \frac{A}{R} c^3 \cos^2 \psi \frac{d}{x_+^3 d\psi} (x_+ \sin \psi). \quad (46)$$

Here \mathfrak{R} is indeed finite at $|\psi| = \pi/2$ if $x_+ \approx O(1/\sqrt{\cos \psi})$, and, for $\psi = 0$,

$$\frac{\mathfrak{R}}{\sqrt{\mu\rho}} = \left(\frac{P}{2\pi\mu}\right)^2 \frac{A_1 c^3}{R_1 x_+^2(0)}, \quad R_1 = 4A_1 B_1 - K_1^2, \quad (47a)$$

$$A_1 = \sqrt{1 - c^2/c_D^2}, \quad B_1 = \sqrt{1 - c^2}, \quad K_1 = c^2 - 2. \quad (47b)$$

Thus, (44) gives the same asymptotic behavior for \mathfrak{R} as that caused by a distributed traction governed by (18) with $\chi = \frac{3}{2}$. Equation (47a) is algebraic, and readily solved. Invariance of \mathfrak{R} leads to the differential equation, for $\psi \neq 0$,

$$\frac{1}{x_+^3} \frac{dx_+}{d\psi} = \frac{A_1 R}{A R_1 \cos^2 \psi} \frac{1}{x_+^2(0)}. \quad (48)$$

Separation of variables (x_+, ψ) is possible in (48), and for $0 < \psi < \pi/2$ leads to

$$\frac{x_+^2(0)}{x_+^2(\psi)} = \frac{2A_1}{R_1} \sin^2 \psi \int_{\psi}^{\pi/2} \frac{d\varphi}{\sin^3 \varphi} \frac{R}{A \cos^2 \varphi}. \quad (49)$$

The integration in (49) produces (E.5) in Appendix E. That formula gives the appropriate result that the right-hand side of (49) is unity for $\psi = 0$, and behaves as $\cos \psi$ for $\psi \rightarrow \pi/2$. Case $-\pi/2 < \psi < 0$ also gives the right-hand side of (E.5), a result that in light of symmetry is also appropriate.

Sample calculation: energy release (rate) criterion

For a solid characterized by $c_D = 2$ and $c_R = 0.932$, (49) and (E.5) are used to calculate dimensionless ratio $x_+(\psi)/x_+(0)$ for $c = 0.1$ and $c = 0.4$ for values $0 \leq \psi \leq 90^\circ$. The results appear in Table 1. Use

c	0.1	0.2	0.3	0.4	0.5	0.6	0.7	0.8
$\beta_1(c)$	0.259	0.3706	0.4631	0.5512	0.6442	0.7534	0.901	1.1579

Table 2. Dimensionless parameter $\beta_1(c)$, $c_R = 0.932$. Note: $\beta_1(0) = \beta_1(c_R) = 0$.

of (4) in (47a) gives a relation in terms of three dimensionless quantities as

$$\sqrt{\Re/PV_S}[\sqrt{\mu/P} x_+(0)] = \frac{\beta_1(c)}{2\pi}, \quad \beta_1(c) = c\sqrt{cA_1/R_1}. \quad (50)$$

Parameter $\beta_1(c)$ defines, therefore, variation in $x_+(0)$ with respect to (dimensionless) crack translation speed c , and calculations are given in Table 2. Combining the entries for $c = 0.1$ and $c = 0.4$ with Table 1 entries leads to schematics of crack edge contour C for $(x_1, x_2) > 0$ ($x > 0$, $0 < \psi < 90^\circ$) in Figure 2. Both contours tend to the rectilinear, but are perturbed by a smooth indentation near the point force location (denoted by \times). It was noted in light of (43) that the strain energy density criterion [Sih 1973] predicts larger values of contour parameter x_+ for $|\psi| \approx \pi/2$ than those predicted by energy release (rate) [Freund 1990]. In view of Figure 2 this implies that the crack edge contour may deviate even more from lines that tend to the rectilinear.

Some comments

This study has produced equations for the radial measure $x_+(\psi)$ from a point on the crack surface to points on the crack edge. Solutions, therefore, define the crack contour. Such equations follow from the criterion for brittle crack growth imposed, and here energy release (rate) and strain energy density are illustrated. Nonlinear first-order differential equations arise in both cases. The strain energy density result is more complicated, because of nonlinearity in both the radial measure and its first derivative.

The case of compressive forces applied to corresponding points on the two crack surfaces is illustrated on the basis of energy release (rate). An analytic solution of the equation, and related calculations, show

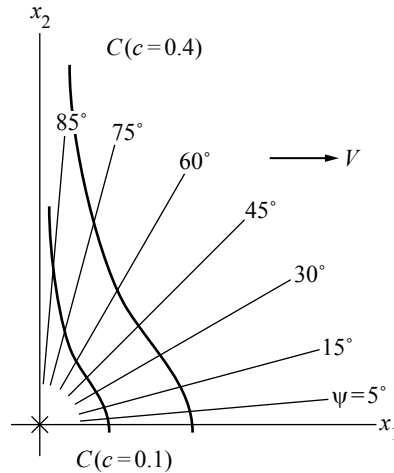


Figure 2. Schematic of crack edge contour, C (drawn to scale).

that the crack contour consists of lines that tend to the rectilinear at great distances from the point forces, but exhibit a pronounced indentation near them. The contours are sensitive to crack growth rate.

The 3D results of this paper are obtained on the assumption that crack growth achieves a dynamic steady state. Nevertheless, they may allow insight into aspects of brittle fracture response that do not arise in a 2D study. On a related note, the analytic results in this paper make use of a “hybrid” form: Cartesian fields are expressed in terms of quasipolar coordinates in the crack plane. The advantages of this are: (a) the solution can be obtained from classical singular integral equations, and (b) some factorization of x_+ and its derivative $dx_+/d\psi$ in the nonlinear equation is possible.

One difficulty, however, with the “hybrid” form is that description of solution behavior in terms of the three fracture modes must be extracted. When crack contour is known or a 2D study is involved, imposition of local Cartesian coordinates that are, respectively, normal to the crack plane, and normal and tangential to the crack edge, is feasible; see, e.g., [Freund 1990]. Based on experience [Brock 2012] with undefined area contours, the author decided that such a coordinate choice could prove to be an analytical stumbling block.

Appendix A

For $x_3 \geq 0(+)$ and $x_3 \leq 0(-)$, respectively,

$$c^2 p_1^2 U^\pm = -\frac{K \hat{U}_3}{2A} \pm (p_1 \hat{U}_1 + p_2 \hat{U}_2), \quad (\text{A.1a})$$

$$c^2 p_1^2 V_1^\pm = p_1 B \hat{U}_3 \pm \left[c^2 p_1^2 \frac{\hat{U}_1}{2} - p_1 (p_1 \hat{U}_1 + p_2 \hat{U}_2) \right], \quad (\text{A.1b})$$

$$c^2 p_1^2 V_2^\pm = p_2 B \hat{U}_3 \pm \left[c^2 p_1^2 \frac{\hat{U}_2}{2} - p_2 (p_1 \hat{U}_1 + p_2 \hat{U}_2) \right]. \quad (\text{A.1c})$$

In (A.1), (B, A) are defined by (9), and

$$K = c^2 p_1^2 - 2D. \quad (\text{A.2})$$

Transforms of traction for $x_3 = 0$ are given by

$$\frac{\hat{\sigma}_{33}}{\mu} = -\frac{\hat{U}_3}{2Ac^2 p_1^2} (4DAB + K^2), \quad (\text{A.3a})$$

$$\frac{\hat{\sigma}_{31}}{\mu} = \frac{p_1}{Bc^2 p_1^2} (K - 2AB)(p_1 \hat{U}_1 + p_2 \hat{U}_2) + \frac{1}{2B} [(p_2^2 - c^2 p_1^2) \hat{U}_1 + p_1 p_2 \hat{U}_2], \quad (\text{A.3b})$$

$$\frac{\hat{\sigma}_{32}}{\mu} = \frac{p_2}{Bc^2 p_1^2} (K - 2AB)(p_1 \hat{U}_1 + p_2 \hat{U}_2) + \frac{1}{2B} [(p_1^2 - c^2 p_1^2) \hat{U}_2 + p_1 p_2 \hat{U}_1]. \quad (\text{A.3c})$$

Appendix B

Consider integrals involving real constants (X, Y) over the entire $\text{Im}(p)$ -axis

$$\frac{1}{2\pi i} \int |p| \left(\frac{\sqrt{-p}}{\sqrt{p}}, 1 \right) \exp(pX - Y\sqrt{-p}\sqrt{p}) \frac{dp}{p} \quad (Y \geq 0). \quad (\text{B.1})$$

As noted in connection with (11) and (12), $\text{Re}(\sqrt{\pm p}) \geq 0$ in the p -plane with branch cuts $\text{Im}(p) = 0$, $\text{Re}(p) < 0$ and $\text{Im}(p) = 0$, $\text{Re}(p) > 0$ respectively. In particular, for $\text{Re}(p) = 0+$ and, respectively, $\text{Im}(p) = q > 0$ and $\text{Im}(p) = q < 0$,

$$\sqrt{-p} = \left| \frac{q}{2} \right|^{1/2} (1 \mp i), \quad \sqrt{p} = \left| \frac{q}{2} \right|^{1/2} (1 \pm i). \quad (\text{B.2})$$

Use of (B.2) reduces (B.1) to

$$\frac{1}{i\pi} \int_0^\infty (\sin qX, \cos qX) \exp(-Yq) dq. \quad (\text{B.3})$$

Integration of (B.3) gives

$$\frac{1}{i\pi} \left[\frac{X}{X^2 + Y^2}, \frac{Y}{X^2 + Y^2} \right] = \frac{1}{i\pi} [\text{Re}, \text{Im}] \frac{1}{X - iY}. \quad (\text{B.4})$$

It is noted that

$$\frac{1}{\pi} \frac{Y}{X^2 + Y^2} \rightarrow \delta(X) \quad (Y \rightarrow 0+). \quad (\text{B.5})$$

Here δ is the Dirac function.

Appendix C

For $x_3 = 0$, $X_- < x < X_+$, $\psi \in \Psi$, i.e., $x_3 = 0$, $(x_1, x_2) \in C$,

$$\frac{\sigma_{33}}{2\mu} = -\frac{G_3}{\pi} (\text{vp}) \int_X \frac{\partial U_3}{\partial x} \frac{d\xi}{\xi - x}, \quad (\text{C.1a})$$

$$\frac{\sigma_{31}}{2\mu} = -\frac{G_1}{\pi} (\text{vp}) \int_X \frac{\partial U_1}{\partial x} \frac{d\xi}{\xi - x} - \frac{G_{12}}{\pi} (\text{vp}) \int_X \frac{\partial U_2}{\partial x} \frac{d\xi}{\xi - x}, \quad (\text{C.1b})$$

$$\frac{\sigma_{32}}{2\mu} = -\frac{G_{21}}{\pi} (\text{vp}) \int_X \frac{\partial U_1}{\partial x} \frac{d\xi}{\xi - x} - \frac{G_2}{\pi} (\text{vp}) \int_X \frac{\partial U_2}{\partial x} \frac{d\xi}{\xi - x}. \quad (\text{C.1c})$$

In (C.1), $U_k = U_k(\xi, \psi)$, (vp) signifies principal value integration, and

$$G_1 = B + \frac{M}{Bc^2}, \quad G_2 = B + \frac{M}{Bc^2} \tan^2 \psi, \quad G_{12} = G_{21} = \frac{M}{Bc^2} \tan \psi, \quad (\text{C.2a})$$

$$G_3 = \frac{R}{Ac^2 \cos^2 \psi}. \quad (\text{C.2b})$$

Terms in (C.2) are defined by (13b) and

$$M = 2N + c^2 \cos^2 \psi, \quad N = 2AB + K, \quad R = 4AB - K^2. \quad (\text{C.3})$$

Appendix D

If $(\sigma_{31}^C, \sigma_{32}^C) = 0$ and $(X_- \rightarrow -\infty, |\psi| < \pi/2)$, strain for $r \approx 0$ is obtained from (44) as

$$e_{11} \approx -\frac{\cos \psi}{\pi^2 \sqrt{2r}} \frac{G}{R} \left(K \frac{A_+}{A_\Phi} + 2AB \frac{B_+}{B_\Phi} \right) \frac{d}{x_+ d\psi} (x_+ \sin \psi), \quad (\text{D.1a})$$

$$e_{22} \approx \frac{\sin \psi}{\pi^2 \sqrt{2r}} \frac{G}{R} \left(K \frac{A_+}{A_\Phi} + 2AB \frac{B_+}{B_\Phi} \right) \frac{d}{x_+ d\psi} (x_+ \cos \psi), \quad (\text{D.1b})$$

$$e_{33} \approx -\frac{A}{\pi^2 \sqrt{2r}} \frac{G}{R} \left(KA \frac{A_+}{A_\Phi} + 2B \frac{B_+}{B_\Phi} \right), \quad (\text{D.1c})$$

$$e_{23} \approx \frac{1}{2\pi^2 \sqrt{2r}} \frac{G}{R} \left(K \frac{A_-}{A_\Phi} + 2B^2 \frac{B_-}{B_+} \right) \sin \psi + \text{sgn}(\phi) \left(K \frac{A_-}{A_\Phi} + 2AB \frac{B_-}{B_\Phi} \right) \frac{d}{x_+ d\psi} (x_+ \cos \psi), \quad (\text{D.1d})$$

$$e_{31} \approx \frac{1}{2\pi^2 \sqrt{2r}} \frac{G}{R} \left(K \frac{A_-}{A_\Phi} + 2B^2 \frac{B_-}{B_\Phi} \right) \cos \psi - \text{sgn}(\phi) \left(K \frac{A_-}{A_\Phi} + 2AB \frac{B_-}{B_\Phi} \right) \frac{d}{x_+ d\psi} (x_+ \sin \psi), \quad (\text{D.1e})$$

$$e_{12} \approx \frac{1}{2\pi^2 \sqrt{2r}} \frac{G}{R} \left(K \frac{A_+}{A_\Phi} + 2AB \frac{B_+}{B_\Phi} \right) \cos \psi \frac{d}{x_+ d\psi} (x_+ \cos \psi) - \sin \psi \frac{d}{x_+ d\psi} (x_+ \sin \psi). \quad (\text{D.1f})$$

The factor G is given by

$$G = \int_X \frac{\sigma_{33}^C dt}{\sqrt{x_+ - t}}. \quad (\text{D.2})$$

Appendix E

In terms of quasipolar coordinates (x, ψ) , (41) gives

$$\sigma_{33}^C = P \frac{\delta(x)}{\pi|x|}, \quad |\psi| < \pi/2. \quad (\text{E.1})$$

Function G in (42) is obtained in terms of representation

$$\sigma_{33}^C = P \frac{\epsilon}{\pi^2 |x| (x^2 + \epsilon^2)} \quad (\epsilon \rightarrow 0). \quad (\text{E.2})$$

Function $F_G(z)$ in the complex z -plane, where $x = \text{Re}(z)$, is defined as

$$F_G(z) = \frac{1}{\sqrt{z^2 - \epsilon_0^2} (z^2 + \epsilon^2) \sqrt{z - x_+}} \quad (\epsilon_0 \approx 0). \quad (\text{E.3})$$

Here $F_G \approx O(z^{-3})$, $|z| \rightarrow \infty$ and exhibits branch cuts on the $\text{Re}(z)$ -axis with branch points $z = (\pm\epsilon_0, x_+)$, and poles $z = \pm i\epsilon$. Thus integration over a closed contour that includes a portion $|z| \rightarrow \infty$, but excludes

the poles and branch cuts, can be performed by residue theory. Setting $\epsilon_0 = 0$ then leads to

$$G = \frac{P}{\pi \alpha \sqrt{2(1+\alpha)}} \frac{1}{x_+^{3/2}}, \quad \alpha = \sqrt{1 + \epsilon^2/x_+^2}, \quad (\text{E.4a})$$

$$G = \frac{P}{2\pi x_+^{3/2}} \quad (\epsilon \rightarrow 0). \quad (\text{E.4b})$$

Use of (E.4) leads to the integral in (49). Introduction of integration variable $u = c \cos \varphi$ gives a form that is readily carried out as

$$\int_{\psi}^{\pi/2} \frac{R \sin^2 \psi}{A \cos^2 \varphi} \frac{d\varphi}{\sin^3 \varphi} = \left(2B - \frac{K_1^2 A}{2A_1^2}\right) \cos \psi + 4(A - B) \frac{\sin^2 \psi}{\cos \psi} \\ + \frac{2K_1}{A_1} \left(1 + \frac{K_1}{A_1^2}\right) \ln \left| \frac{A + A_1 \cos \psi}{A - A_1 \cos \psi} \right| \sin^2 \psi + 2 \left(B_1 + \frac{1}{2B_1}\right) \ln \left| \frac{B + B_1 \cos \psi}{B - B_1 \cos \psi} \right| \sin^2 \psi. \quad (\text{E.5})$$

The right-hand side behaves as $\cos \psi$ for $\psi = \pi/2$, and for $\psi = 0$ gives $R_1/2A_1$.

References

- [Achenbach 1975] J. D. Achenbach, *Wave propagation in elastic solids*, North-Holland Series in Applied Mathematics and Mechanics, Elsevier, Amsterdam, 1975.
- [Achenbach and Brock 1973] J. D. Achenbach and L. M. Brock, “On quasistatic and dynamic fracture”, pp. 529–541 in *Proceedings of an international conference on dynamic crack propagation*, edited by G. C. Sih, Springer Netherlands, 1973.
- [Brock 1999] L. M. Brock, “Effects of mixed-mode and crack surface convection in rapid crack growth in coupled thermoelastic solids”, *Journal of Applied Mechanics* **67**:1 (10/12 1999), 59–65.
- [Brock 2012] L. M. Brock, “Two cases of rapid contact on an elastic half-space: sliding ellipsoidal die, rolling sphere”, *Journal of mechanics of materials and structures* **7**:5 (2012), 469–483.
- [Brock 2014a] L. M. Brock, “The rigid die on a half-space with thermal relaxation and convection: influence of sliding speed, die temperature, and geometry”, *Journal of Thermal Stresses* **37**:7 (2014), 832–851.
- [Brock 2014b] L. M. Brock, “Sliding of a cup-shaped die on a half-space: influence of thermal relaxation, convection and die temperature”, *Journal of mechanics of materials and structures* **9**:3 (2014), 347–363.
- [Brock 2015] L. M. Brock, “Rapid sliding on a thermoelastic half-space: rigid die with two contact surfaces”, *Journal of thermal stresses* (2015).
- [Freund 1990] L. B. Freund, *Dynamic fracture mechanics*, Cambridge Monographs on Mechanics and Applied Mathematics, Cambridge University Press, 1990.
- [Griffith 1921] A. A. Griffith, “The phenomena of rupture and flow in solids”, *Philosophical Transactions of the Royal Society of London A: Mathematical, Physical and Engineering Sciences* **221**:582–593 (1921), 163–198.
- [Sih 1973] G. C. Sih, “Energy-density concept in fracture mechanics”, *Engineering Fracture Mechanics* **5**:4 (1973), 1037–1040.
- [Sneddon 1972] I. N. Sneddon, *The use of integral transforms*, McGraw-Hill, New York, 1972.

Received 27 Sep 2014. Accepted 16 Dec 2014.

LOUIS MILTON BROCK: louis.brock@uky.edu

Department of Mechanical Engineering, University of Kentucky, 265 RGAN, Lexington, KY 40506-0503, United States

JOURNAL OF MECHANICS OF MATERIALS AND STRUCTURES

msp.org/jomms

Founded by Charles R. Steele and Marie-Louise Steele

EDITORIAL BOARD

ADAIR R. AGUIAR	University of São Paulo at São Carlos, Brazil
KATIA BERTOLDI	Harvard University, USA
DAVIDE BIGONI	University of Trento, Italy
IWONA JASIUK	University of Illinois at Urbana-Champaign, USA
THOMAS J. PENCE	Michigan State University, USA
YASUhide SHINDO	Tohoku University, Japan
DAVID STEIGMANN	University of California at Berkeley

ADVISORY BOARD

J. P. CARTER	University of Sydney, Australia
D. H. HODGES	Georgia Institute of Technology, USA
J. HUTCHINSON	Harvard University, USA
D. PAMPLONA	Universidade Católica do Rio de Janeiro, Brazil
M. B. RUBIN	Technion, Haifa, Israel

PRODUCTION production@msp.org

SILVIO LEVY Scientific Editor

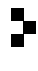
Cover photo: Ev Shafir

See msp.org/jomms for submission guidelines.

JoMMS (ISSN 1559-3959) at Mathematical Sciences Publishers, 798 Evans Hall #6840, c/o University of California, Berkeley, CA 94720-3840, is published in 10 issues a year. The subscription price for 2015 is US \$565/year for the electronic version, and \$725/year (+\$60, if shipping outside the US) for print and electronic. Subscriptions, requests for back issues, and changes of address should be sent to MSP.

JoMMS peer-review and production is managed by EditFLOW[®] from Mathematical Sciences Publishers.

PUBLISHED BY

 **mathematical sciences publishers**
nonprofit scientific publishing

<http://msp.org/>

© 2015 Mathematical Sciences Publishers

Journal of Mechanics of Materials and Structures

Volume 10, No. 1

January 2015

Flexural behavior of functionally graded slender beams with complex cross-section GHOLAMALI SHARIFISHOURABI, AMRAN AYOB, SCOTT GOHERY, MOHD YAZID BIN YAHYA, SHOKROLLAH SHARIFI and ZORA VRCELJ	1
Response of submerged metallic sandwich structures to underwater impulsive loads SIDDHARTH AVACHAT and MIN ZHOU	17
Thermal and magnetic effects on the vibration of a cracked nanobeam embedded in an elastic medium DANILO KARLIČIĆ, DRAGAN JOVANOVIĆ, PREDRAG KOZIĆ and MILAN CAJIC	43
Contours for planar cracks growing in three dimensions LOUIS MILTON BROCK	63
Mechanical degradation of natural fiber reinforced composite materials under constrained swelling YIHUI PAN and ZHENG ZHONG	79
On the occurrence of lumped forces at corners in classical plate theories: a physically based interpretation LAURA GALUPPI and GIANNI ROYER-CARFAGNI	93